Cosmic Dawn Intensity Mapper:
Spacecraft and Mission Design for a Probe-Class Space Telescope

Philip Linden[1,†], Michael Zemcov[2]

[1]*Department of Mechanical Engineering, Kate Gleason College of Engineering, Rochester Institute of Technology, Rochester, NY 14623, USA, pjl7651@rit.edu*

[2]*Center for Detectors, School of Physics and Astronomy, Rochester Institute of Technology, Rochester, NY 14623, USA, zemcov@cfd.rit.edu*

Cosmic Dawn Intensity Mapper (CDIM) is a Probe-class near-IR space telescope with the scientific goal of conducting large spectro-imaging surveys over a five-year mission in the next decade. A high-level system architecture was designed to identify key features and technologies aboard the CDIM spacecraft in preparation for more detailed studies such as a Team-X session at NASA Jet Propulsion Laboratory.

Keywords: spacecraft, telescope, system, cryogenic, infrared, design.
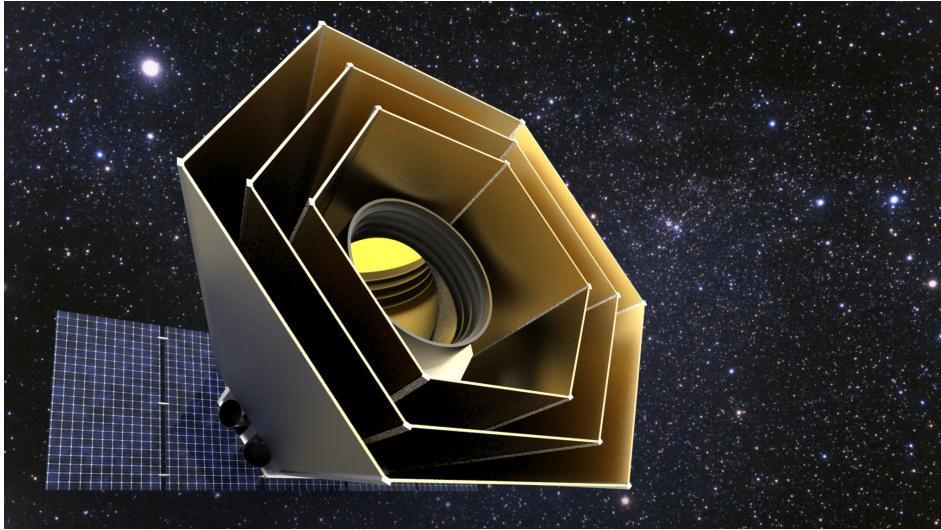
1. Introduction

Fig. 1. An artistic rendition of the Cosmic Dawn Intensity Mapper stationed at Sun-Earth L_2.

The Cosmic Dawn Intensity Mapper (CDIM) is a concept for a Probe-class 1.5 m aperture telescope, passively cooled to 45 K, with an actively cooled 6×6 detector array that utilizes linear variable filters (LVFs) (Cooray *et al.*, 2016) capable of three-dimensional spectro-imaging observations over the wavelength range of 0.75 to 7.5 μm at a spectral resolving power R= 500. CDIM has a 10 deg^2 instantaneous field of

---

[†]Corresponding author.

Table 1.   Critical design requirements for the CDIM spacecraft.

Spacecraft Design Driver	Impact	Target
Cost	Science capability, instrument architecture	less than \$1 B
Mass	Launch vehicle	less than $1000\,\text{kg}$
Temperature (OTA)	Passive radiator	45 K
Temperature (Detector)	Cryocooler	35 K
Pointing Requirements	Attitude control system	less than 0.5 arcsec
Lifetime	Redundancy, RCS propellant	5 years
Orbit	Solar array, thermal management, launch vehicle, telemetry	Sun-Earth L_2

view (FoV) atop a focal plane of thirty-six 2048×2048 detectors. The survey strategy using spacecraft operations following a shift and stare mode will result in 1360 independent narrow-band spectral images of the sky on a given location. Surveys are planned to span from $25\,\text{deg}^2$ up to $1000\,\text{deg}^2$ over a five year lifetime in an orbit about Sun-Earth Lagrange point L_2.

Although Wide Field Infrared Survey Telescope (WFIRST) will be capable of $3400\,\text{deg}^2$ wide area surveys, its spectroscopy is limited to $2\,\mu\text{m}$, limiting the selection of galaxies it is able to observe (Green *et al.*, 2012). While James Webb Space Telescope (JWST) is capable of targeted spectroscopy studies of galaxies present in reionization and surveys $10\,\text{armin}^2$ for reionization galaxies (Gardner *et al.*, 2006), CDIM will make use of tomographic intensity mapping of spectral emission lines to study the aggregate statistical properties of the sources and their spatial distribution. The intensity of the Lyα and Hα lines, combined with others, will also provide critical clues to the formation of metals in the universe (Cooray *et al.*, 2016).

Probe-class missions occupy a role on a larger scale than Discovery missions, such as Kepler and Dawn, but not as large as Flagship missions such as JWST. Such missions are intended to be PI-led scientific investigations rather than general observatories, and have a firm \$1B cap (Wiseman *et al.*, 2015). Critical design requirements to achieve CDIM's science goals as a Probe-class mission are summarized in Table 1.

2. Optical Telescope Assembly

Preliminary explorations indicate that a 1.3–1.5m aperture off-axis primary mirror cooled to 45 K is required to meet CDIM's spectro-imaging requirements (Cooray *et al.*, 2016). The primary mirror is notionally assumed to be constructed from light-weighted Corning (ultra-low expansion) silica-titania glass with a honeycomb core and a gold-deposition surface coating. For this type of mirror, the estimated mass is in the neighborhood of 200 kg.

HgCdTe infrared detectors meet CDIM design goals of operating at cryogenic temperatures, low in cost, and, of course, sensitive in near-IR. Several different off-the-shelf CMOS detectors satisfy CDIM's spatial resolution, wavelength range, and sensitivity requirements. These detectors range in technology-readiness-level (TRL), but all are sufficiently developed to be considered for the 2020 Decadal and will be demonstrated on missions such as NEOCam, SPHEREx, and JWST (Doré *et al.*, 2014; Gardner *et al.*, 2006).

Insert table of detectors. Teledyne H2RG-18 HyViSI detectors offer a 2048×2048 pixel array format at a pixel pitch of $18\,\mu\text{m}$ (Bai *et al.*, 2008). CDIM will utilize 36 detectors in a close-packed, 6×6 mosaic focal plane assembly (FPA). In the expected normal operating mode, each detector dissipates less than $4\,\text{mW}$, for a total power dissipation of less than $150\,\text{mW}$ for the full array.

Linear-variable filters (LVFs) will be placed just above the detectors to provide spectral dispersion for spectrometry. LVFs are simple, space-qualified solutions to permit spectral data cubes between 0.75–7.5μm that are commercially available and significantly lower in cost than more complex systems. Citation needed.

CDIM optics, instruments, and focal plane will be housed in a light-tight box to minimize signal contamination from stray light. The light-tight box is constructed of gold-plated aluminum. The optical telescope assembly (OTA) as a whole is estimated to have a mass of 200–250kg.

3. Thermal Design

CDIM will employ both passive and active thermal regulation systems. By using passive radiators in tandem with an active cryocooler, the static OTA heat load can be dissipated by the lightweight radiator and a smaller cryocooler may be used to only cool the detector array rather than the whole OTA mass plus FPA. Passive cooling is used to cool the OTA and FPA from solar radiation, while active cooling regulates heat dissipated by active detectors.

The OTA is cooled to 45 K to reduce background photon load in the near-IR. Passive thermal regulation is maintained using a multi-stage V-groove radiator, which bounces radiative heat into the 3 K background of space (Bard, 1987).
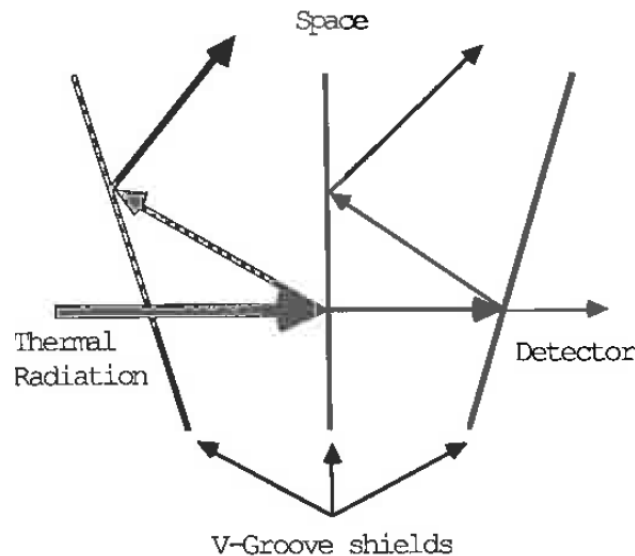

Figure 4. V-Groove shielding concept.

Fig. 2. Low emmissivity, high specular surface vanes are nested at a slight angle to reflect thermal radiation into space (Rasbach, 1988). Replace this figure with a powerpoint graphic.

V-groove radiators have been demonstrated in passive cryogenic radiators up to 4 K with Planck, SPIRIT, and Spitzer (warm mission). Like Planck, the active coolers are also pre-cooled to less than 50 K this way. Citation needed: Planck CalTech Paper. In order to achieve passive cooling from a baseline temperature of 300 K at Sun-Earth Lagrange point L$_2$, a x-stage V-groove radiator with an area of x m^2 is required. Since CDIM may be at various angles of incidence to solar radiation as it surveys the sky, the V-groove radiator fins will extend outward, more like SPHEREx than Planck.

CDIM's thermal requirement to have the detector array actively cooled to 35 K in order to reduce thermal noise can be met by a commercially available mechanical cryocooler. Stirling-cycle mechanical refrigerators are low-vibration, high-reliability, and lightweight active cryocooling systems that have significant heritage in space applications. One candidate system is Raytheon's PSC 1-stage Stirling cryocooler, capable of cooling a 1.2 W parasitic heat load to 35 K. This cryocooler is 18.6 kg and requires 88 W of input power (Donabedian *et al.*, 2003).

4. Attitude Determination and Control

To conduct a survey, the spacecraft must first understand its orientation and then act to align itself with a given area of the sky. Redundant systems of varying levels of fidelity are included to allow CDIM to operate in different power states. Low-fidelity attitude determination sensors such as sun sensors are cheap,

accurate to less than one degree, and lightweight.

High-fidelity attitude determination is conducted by off-the-shelf star tracking cameras. Star trackers identify constellations in their field of view to determine the spacecraft's heading to within 0.25 arcseconds. Identify candidate star trackers.

In a heliocentric orbit, the primary disturbance to the spacecraft's heading is solar radiation pressure (SRP). At L_2, solar radiation pressure presents itself as torque on the spacecraft with a maximum on the order of 10^{-5} N m.

Cold-gas or hydrazine thrusters will be used for orbit station-keeping as well as momentum management. A desired heading is maintained by the spacecraft using a 3-axis zero-momentum inertial system, whereby the error in heading due to SRP is cancelled out by spinning up or slowing down reaction wheels. Reaction wheel systems are capable of torques ranging from .01 to 1 N m and store 0.4 to 3000 N m s of practical momentum (Wertz *et al.*, 2015). Power consumption varies with reaction wheel speed, with a maximum estimate of roughly 100 W. After some time the inertial attitude control may become saturated. Desaturation is managed by engaging station-keeping thrusters for short periods of time. Additionally, these thrusters will be used to maintain an orbit at L_2 as it is an inherently unstable orbit.

5.   Flight Computer

CDIM is capable of autonomous operation and system diagnostics. Nominal operation includes maintaining an attitude during imaging, capturing images, and downlinking data to Earth. Images will be processed on-board CDIM using an algorithm demonstrated by SPHEREx (Zemcov *et al.*, 2016).

6.   Telemetry

Typically for high-Earth and deep-space missions, the X-Band Space Science frequency band is used for uplink and downlink between the spacecraft and Ground Stations. Thus, high-gain antennas are best suited for both links (Wertz *et al.*, 2015).

A survey conducted by CDIM will generate 168.39 Gb of data per day employing on-board data processing akin to SPHEREx (Zemcov *et al.*, 2016). With a compression ratio of 2.5:1, CDIM will downlink a total of 63.7 Gb/day during a survey. Transmission rates are dependent on the total time available for CDIM to send data to a ground station. For example, the spacecraft could transmit continuously at a very low transfer rate, or send larger volumes of data once per day over 1 hour at the expense of a higher transfer rate. Example calculation of data to downlink 1 day in 1 hr.

Uplinks will follow standard protocols and do not require transmitting large volumes or particularly fast transfer rates.

Table 2.   For redundancy, CDIM is outfitted with multiple communication modes. Downlink transfer rates reflect estitmates based on the target of 63.7 Gb/day. Typical data transfer rates are outlined for uplinks (Wertz *et al.*, 2015).

Mode	Uplink	Downlink
Emergency	7.8 bps	5–10bps
Engineering data	15.6–2000kbps	Up to 10 bps
Science data	15.6–2000kbps	0.74 Mbps (continuous) or 17.7 Mbps (1 hour per day)

Identify candidate telemetry systems. The CDIM telemetry system, including antenna and power converter, are roughly 2 kg.

7.   Power

Since CDIM will be located at L_2, it is exposed to constant and significant solar flux. All power generation will come from an array of photovoltaic cells facing the sun. While the array may be fixed, the required

area of the array is minimized if the cells are able to adjust to account for different incident angles to the sun. The array will deploy after the launch and orbital insertion phases of the mission.

Based on a rough power budget and the spacecraft's position at L_2, the array must be min x–max $x\text{m}^2$ in area to sustain operation. The dark side of the array acts as a radiator to contribute to the thermal regulation of the spacecraft bus.

Identify candidate systems.

8. Structure

The spacecraft bus houses all non-instrumentation systems including the cryocooler, ADCS, telemetry, processing, and power modules. The bus will also include hard points for integration with the launch vehicle. The CDIM spacecraft bus will not feature novel technology. Rather it will leverage high TRL or off-the-shelf components.

9. Orbit

CDIM will orbit around Sun-Earth Lagrange point L_2 since it allows the spacecraft to be oriented such that half of the celestial sphere is visible at all times, and the spacecraft may oppose the Sun, Earth, and Moon concurrently and at all times. This also leads to a very thermally stable environment. L_2 is near enough to Earth (roughly 1.5 million km) so that CDIM may communicate with ground stations without the Deep Space Network, and maintains near-constant communications geometry (Canalias *et al.*, 2004).
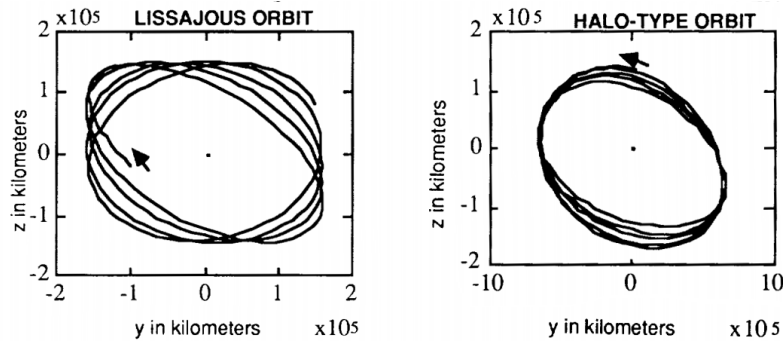

Fig. 3. *Left:* Orthographic view of a quasi-periodic Lissajous orbit. *Right:* Orthographic view of a periodic halo orbit. (Gordon, 1993)

Around L_2, two types of orbit are considered: Lissajous and halo-type orbits. Lissajous orbits are quasi-periodic but may be smaller in radius than periodic halo orbits. Halo orbits are more costly to achieve in terms of delta-v, or energy to transfer into such trajectory. Station-keeping costs are not significantly different between the two orbits (Gordon, 1993). As such, CDIM may enter a Lissajous orbit around L_2 similar to the orbits of JWST and Herschel missions.

10. Launch Vehicle

CDIM will be comfortably within the mass and spatial limits of both currently available and development launch vehicles capable of delivering payloads to Sun-Earth Lagrange Point L_2. Future launch vehicles will be more than capable of delivering CDIM to L_2, and industry trends indicate that heavy and super-heavy vehicles will continue to come online by the time CDIM launches.

Due to the rigorous launch environment, CDIM solar panels and passive radiators will not be deployed until CDIM is delivered to a transfer orbit en route to L_2.

11. Cost Estimation

The overall cost of a space telescope may be broken down on the subsystem level. All conclusions based on statistical analysis are only as good as their databases. Fiscal data, such as what is required for proper

Table 3.   Available launch vehicle configurations and their capabilities to send NASA payloads to L_2 (Rioux, 2016; Space Launch Report).

Vehicle	Payload to L_2	Fairing size	Cost[†]
Falcon 9 v1.1	2900 kg	5.2 × 13.1 m	$97M
Falcon Heavy[*]	14 000 kg	5.2 × 13.1 m	$120M
Atlas V 551	6100 kg	4.2 × 10.0 m 5.1 × 11.0 m	$153M
Ariane V	6600 kg	5.4 × 12.7 m 5.4 × 13.8 m 5.4 × 17.0 m	$165M $220M
Delta IV Heavy	9800 kg	5.0 × 14.3 m 5.0 × 19.1 m	$375M

[†] Launch costs may be higher due to NASA mandated oversight and testing.
[*] Costs and capacities are representative of design specifications for launch vehicles that are currently in development.

analysis, is scarce. Estimations are made with engineering judgement based on available data.

To estimate the cost of the CDIM mission, costs are separated into drivers of the *mission cost*, which includes hardware, development, ground support, integration, testing, science, and management. Existing generalized parametric cost estimation approaches identify key cost drivers for mission cost (Stahl *et al.*, 2013; Bely, 2011), but do not take labor or overhead costs into account. Overhead and labor costs are included in a more robust model for *total cost*, where:

$$\text{Total Cost} = (1.5) \times \text{Mission Cost} \tag{1}$$

Stahl *et al.* present an approach to estimating OTA cost based on correlations with data on flown space telescope missions. CDIM's projected costs may be obtained from these findings with engineering judgement, knowing that the data is drawn from a relatively small sample set. Thus, an OTA aperture diameter of 1.5 m yields a median OTA cost of $58.2M. Since OTA cost is found, estimates for other cost drivers may be obtained from relative cost values.

The most robust model for the CDIM mission predicts its total cost to be $684.7M, and even the more conservative model predicts CDIM costing to fall under $800M. The CDIM mission has significant margin under the $1B cap for Probe-class missions.

| | | Est. Cost | |
Driver	% Mission Cost	1.3 m	1.5 m
OTA	13 %	$48.0M	$58.2M
Spacecraft	20 %	$76.8M	$91.3M
Instruments	15 %	$57.6M	$69.8M
Ground Support	5 %	$18.8M	$22.8M
Integration & Testing	7 %	$25.6M	$31.0M
Systems Engineering	4 %	$16.0M	$19.4M
Management	4 %	$16.0M	$19.4M
R&D	21 %	$80.0M	$97.0M
Science Team	10 %	$37.6M	$45.6M
Mission Cost		$188.2M	$456.5M
Labor & Overhead		$376.5M	$228.2M
Total Cost		$564.7M	$684.7M

Table 4.   CDIM total cost breakdown by driver. Make total cost less dependent on OTA cost. Ground support and science costs shouldnt rise so much along with OTA cost. Maybe just show one diameter and hide the other graph.
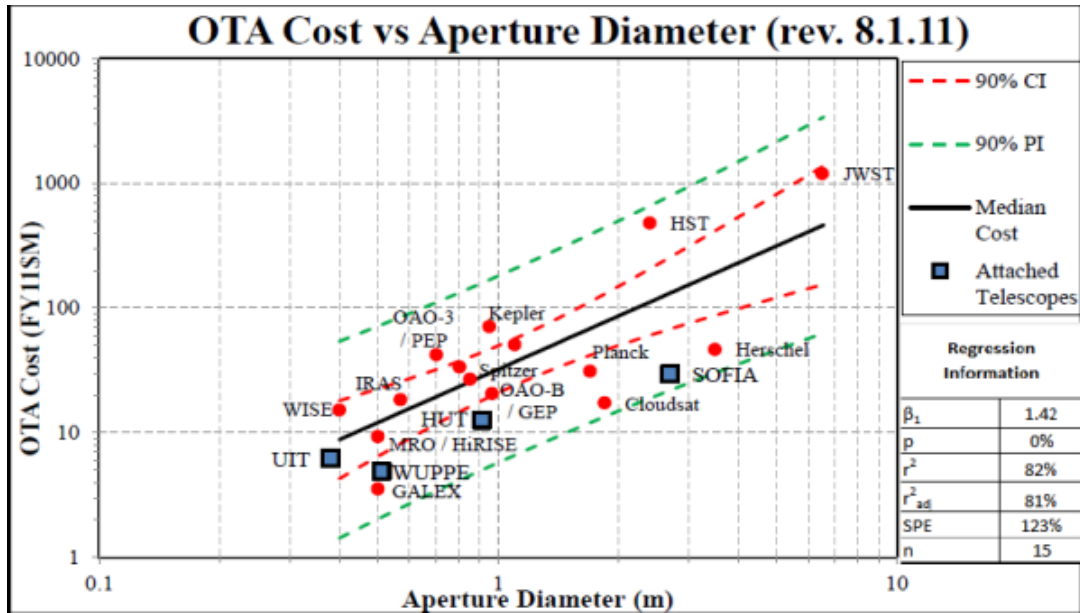

Fig. 4.   Optical Telescope Assembly vs. cost correlation (Stahl *et al.*, 2013). Given a target OTA aperture diameter of 1.5 m for CDIM, a reasonable estimate of OTA cost is obtained from the median cost trendline.
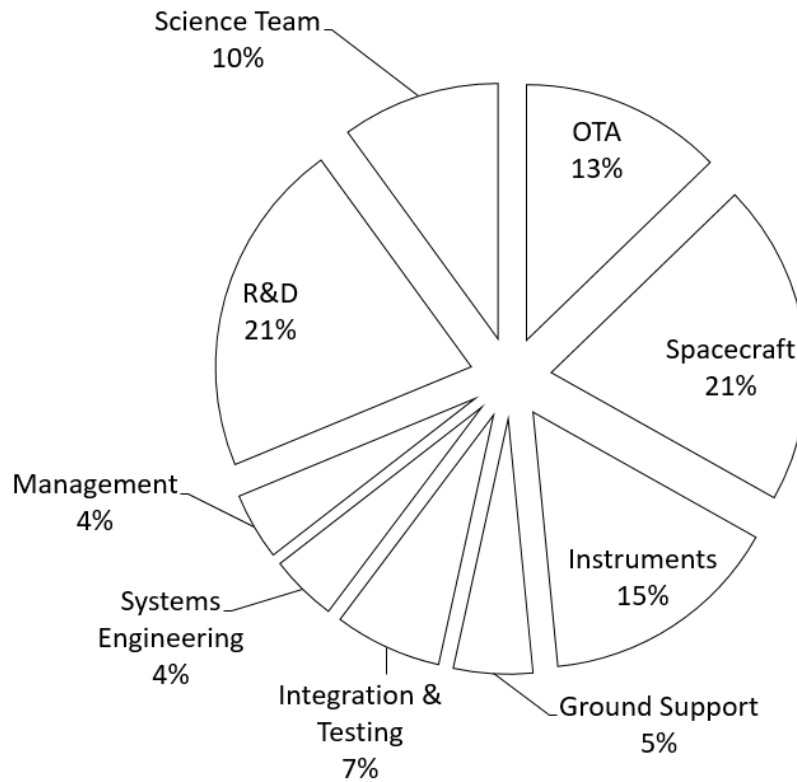
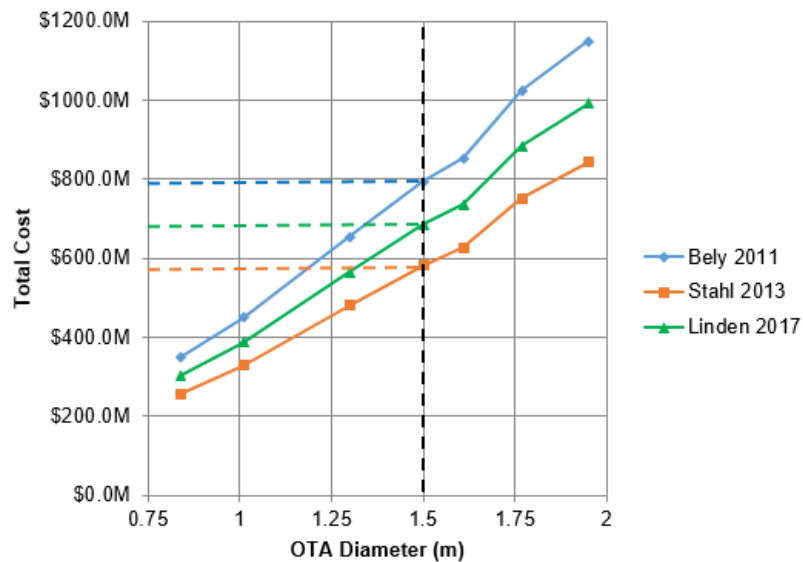Fig. 5.   CDIM estimated cost breakdown in percent of mission cost.

Fig. 6.   CDIM total cost relation to OTA aperture diameter under various cost models. The model described here is robust and presents a conservative estimate compared to similar models by Bely and Stahl *et al.*, after a total cost approximation is applied following Equation 1.
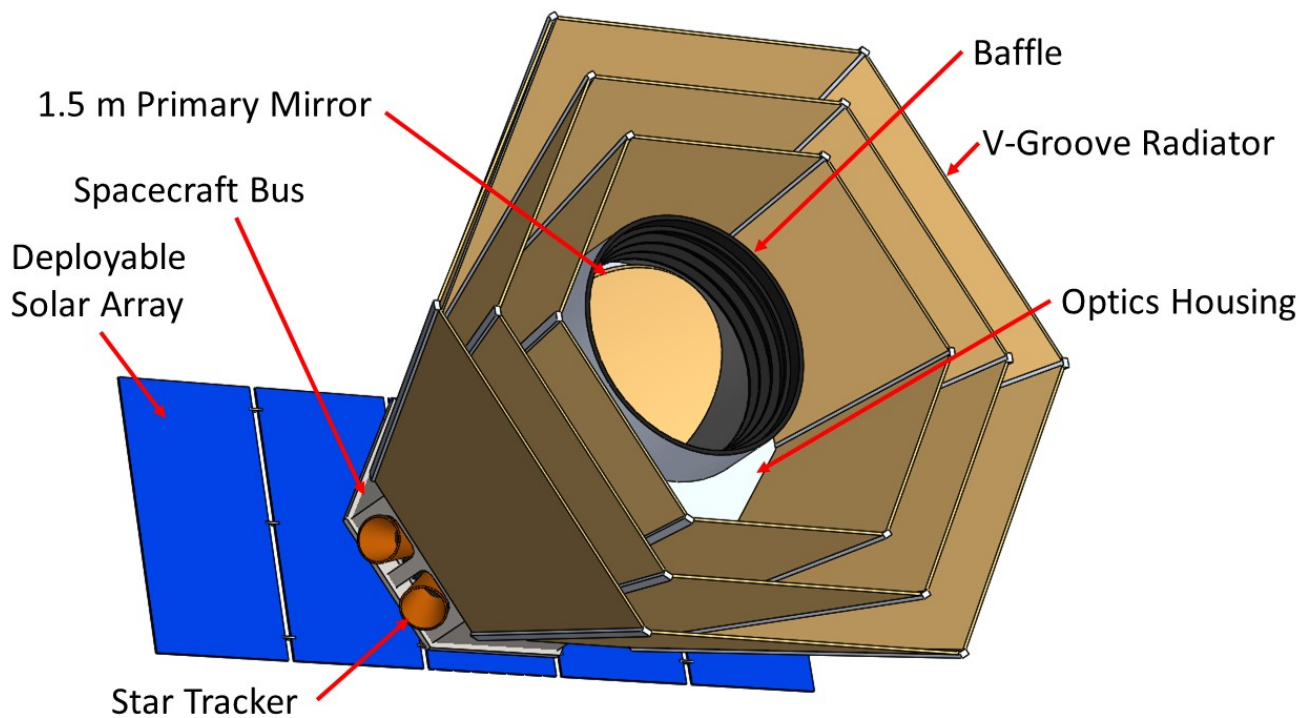
12. Conclusion

Fig. 7. CDIM consists of a passively cooled 1.5 m aperture OTA, actively cooled focal plane, and off-the-shelf spacecraft components where applicable. Add cutaway view.

Acknowledgments

References

Bai, Y., Bajaj, J., Beletic, J. W., Farris, M. C., Joshi, A., Lauxtermann, S., Petersen, A. & Williams, G. [2008] "Teledyne imaging sensors: silicon cmos imaging technologies for x-ray, uv, visible, and near infrared," doi: 10.1117/12.792316, URL http://dx.doi.org/10.1117/12.792316.

Bard, S. [1987] *Journal of Spacecraft and Rockets* **24**, 193, doi:10.2514/3.25898.

Bely, P.-Y. [2011] *The Design and Construction of Large Optical Telescopes* (Springer).

Canalias, E., Gomez, G., Marcote, M. & Masdemont, J. [2004] *ESA Advanced Concept Team* .

Cooray, A., Bock, J., Burgarella, D., Chary, R., Chang, T.-C., Doré, O., Fazio, G., Ferrara, A., Gong, Y., Santos, M., Silva, M. & Zemcov, M. [2016] *ArXiv e-prints* .

Donabedian, M., of Aeronautics, A. I., Astronautics & (Firm), K. [2003] *Spacecraft thermal control handbook* (Aerospace Press, El Segundo, Calif), ISBN 9781884989148.

Doré, O., Bock, J., Capak, P., de Putter, R., Eifler, T., Hirata, C., Korngut, P., Krause, E., Masters, D., Raccanelli, A. *et al.* [2014] *arXiv preprint arXiv:1412.4872* .

Gardner, J. P., Mather, J. C., Clampin, M., Doyon, R., Greenhouse, M. A., Hammel, H. B., Hutchings, J. B., Jakobsen, P., Lilly, S. J., Long, K. S., Lunine, J. I., Mccaughrean, M. J., Mountain, M., Nella, J., Rieke, G. H., Rieke, M. J., Rix, H.-W., Smith, E. P., Sonneborn, G., Stiavelli, M., Stockman, H. S., Windhorst, R. A. & Wright, G. S. [2006] *Space Science Reviews* **123**, 485, doi:10.1007/s11214-006-8315-7, URL http://dx.doi.org/10.1007/s11214-006-8315-7.

Gordon, S. C. [1993] .

Green, J., Schechter, P., Baltay, C., Bean, R., Bennett, D., Brown, R., Conselice, C., Donahue, M., Fan, X., Gaudi, B. S., Hirata, C., Kalirai, J., Lauer, T., Nichol, B., Padmanabhan, N., Perlmutter, S., Rauscher, B., Rhodes, J., Roellig, T., Stern, D., Sumi, T., Tanner, A., Wang, Y., Weinberg, D., Wright, E., Gehrels, N., Sambruna, R., Traub, W., Anderson, J., Cook, K., Garnavich, P., Hillenbrand, L., Ivezic, Z., Kerins, E., Lunine, J., McDonald, P., Penny, M., Phillips, M., Rieke, G., Riess, A., van der Marel, R., Barry, R. K., Cheng, E., Content, D., Cutri, R., Goullioud, R., Grady, K., Helou, G., Jackson, C., Kruk, J., Melton, M., Peddie, C., Rioux, N. & Seiffert, M. [2012] "Wide-field infrared survey telescope (wfirst) final report," .

Rasbach, C. [1988] *26th Aerospace Sciences Meeting* doi:10.2514/6.1988-557.

Rioux, N. [2016] "Getting to orbit: Launch vehicles," .

Space Launch Report [2017] "Launch vehicle datasheets," http://www.spacelaunchreport.com/.

Stahl, H. P., Henrichs, T., Luedtke, A. & West, M. [2013] *Optical Engineering* **52**, 091805, doi:10.1117/1.OE.52.9.091805, URL http://dx.doi.org/10.1117/1.OE.52.9.091805.

Wertz, J. R., Everett, D. F. & Puschell, J. J. [2015] *Space mission engineering: the new SMAD* (Microcosm Press).

Wiseman, J., Clampin, M., Danchi, W., Mather, J., Oegerle, W., Barry, R., Traub, W., Stapelfeldt, K., Lissauer, J., Borucki, W., Greene, T., Bennett, D. & Johnston, K. [2015] "Space-based "probe class" missions for exoplanet research," https://science.gsfc.nasa.gov/667/whitepapers/ProbeClassMissions_whitepaper.pdf.

Zemcov, M., Crill, B., Ryan, M. & Staniszewski, Z. [2016] doi:10.1142/S2251171716500070.